

Supplementary Information

A porous graphene - NiFe₂O₄ nanocomposite with high electrochemical performance and high cyclic stability for energy storage applications

Meenaketan Sethi[†], U. Sandhya Shenoy[‡], D Krishna Bhat^{†,*}

[†]Department of Chemistry, National Institute of Technology Karnataka, Surathkal,
Mangalore - 575025, India

[‡]Department of Chemistry, College of Engineering and Technology, Srinivas University, Mukka,
Mangalore - 574146, India

Corresponding author* email: denthajekb@gmail.com

Methods

1. Electrochemical analysis of the electrode

The equations followed for estimation of specific capacitance ($F g^{-1}$), specific capacity ($C g^{-1}$), energy density ($W h kg^{-1}$), and power density ($W kg^{-1}$) are given below.

The specific capacitance values from the CV graphs were calculated using the equation 1

$$C_s = \frac{\int_{V_1}^{V_2} I(V) dV}{mv(V_2 - V_1)} \quad (1)$$

where, C_s is specific capacitance ($F g^{-1}$), I (A) is the cathodic or anodic current, dV (V) is the operated potential window, v ($V s^{-1}$) is the applied scan rate, m (g) is the deposited mass on Ni sheet.

where, C_s is specific capacitance ($F g^{-1}$), I (A) is the cathodic or anodic current, (V) dV is is the operated potential window, v ($V s^{-1}$) is the applied scan rate, m (g) is the deposited mass on Ni sheet.

The specific capacitance ($F g^{-1}$) values from the GCD graphs were calculated using the equation 2.

$$C_s = \frac{I \times \Delta t}{m \times \Delta V} \quad (2)$$

where, C_s = specific capacitance ($F g^{-1}$), I/m ($A g^{-1}$) is the applied current density, Δt (s) is the discharging time, ΔV (V) is the maximum potential window to discharge the cell.

The specific capacity Q_s ($C g^{-1}$) was calculated by using the equation (3), since NF exhibits battery type behavior.

$$Q_s = \frac{I \times \Delta t}{m} \quad (3)$$

The energy density and power density for the prepared electrode were calculated according to equation 4 and 5, respectively.

$$\text{Energy density (Wh kg}^{-1}\text{)} = \frac{1}{2} C_s \Delta V^2 \frac{1000}{3600} \quad (4)$$

$$\text{Power density (W kg}^{-1}\text{)} = \frac{E}{t_d} \times 3600 \quad (5)$$

where, C_s = specific capacitance (F g^{-1}), ΔV (V) is the maximum potential window, E is the energy density and t_d (s) is the discharging time.

2. Electrochemical analysis of the supercapacitor cell

The specific capacitance (F g^{-1}) values from the CV graphs were calculated using equation 6.

$$C_s = \frac{2 A}{m v \Delta V} \quad (6)$$

where, C_s = specific capacitance (F g^{-1}), A is the integrated area of the CV curve, v (V s^{-1}) is the applied scan rate, m (g) is the deposited mass on one single carbon paper, and ΔV (V) is the operated potential window. A factor of 2 is multiplied due to the formation of series capacitance in a symmetrical supercapacitor device.

The specific capacitance (F g^{-1}) and energy density values from the GCD graphs were calculated using the equation 7 and 8.

$$C_s = 2 \times \frac{I \times \Delta t}{m \times \Delta V} \quad (7)$$

$$\text{Energy density (Wh kg}^{-1}\text{)} = \frac{1}{8} C_s \Delta V^2 \frac{1000}{3600} \quad (8)$$

where, C_s = specific capacitance (F g^{-1}), ΔV (V) is the maximum potential window, E is energy density and t_d (s) is the discharging time.

The specific capacitance (F g^{-1}) was also determined through integral method as shown in equation 9.

$$C_s = \frac{2 \times I \int V dt}{m \Delta V^2} \quad (9)$$

Specific capacity from GCD curve was calculated using equation 10,

$$Q_s = C \times \Delta U \quad (10)$$

Q_s is the specific capacity, C is the capacitance obtained from GCD curve and ΔU is the potential window.

The coulombic efficiency (%) was calculated using equation 11

$$\eta (\%) = \frac{\Delta t_d}{\Delta t_c} \times 100 \quad (11)$$

Δt_d , Δt_c are the discharging time and charging time, respectively.

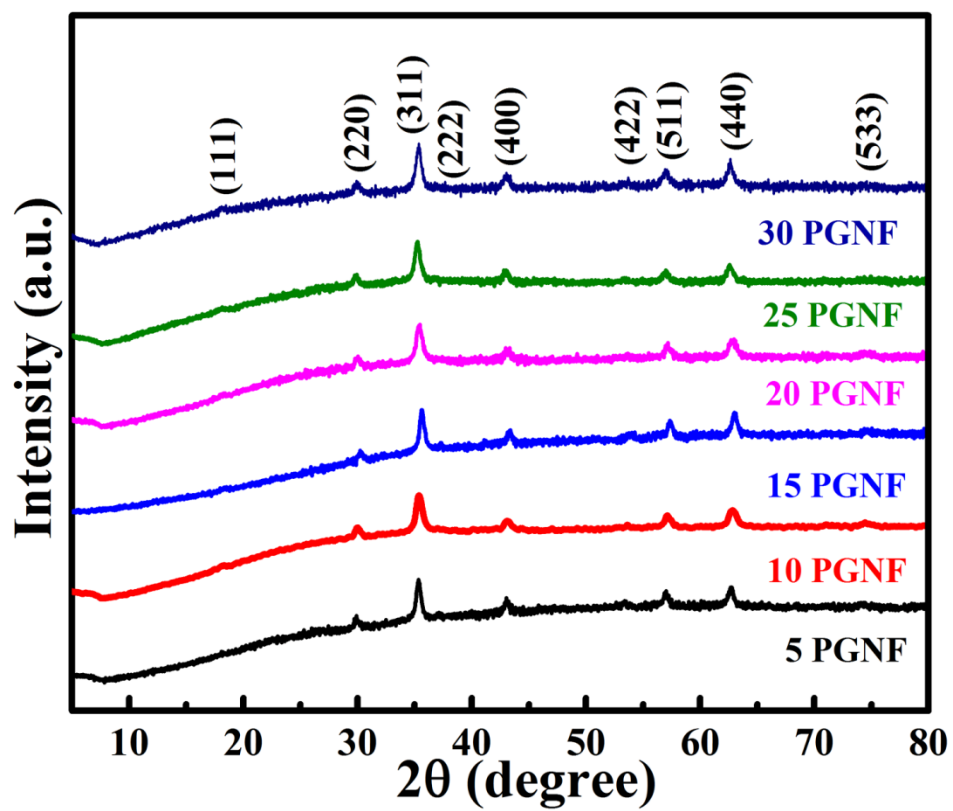


Figure S1. XRD patterns of PGNF nanocomposites.

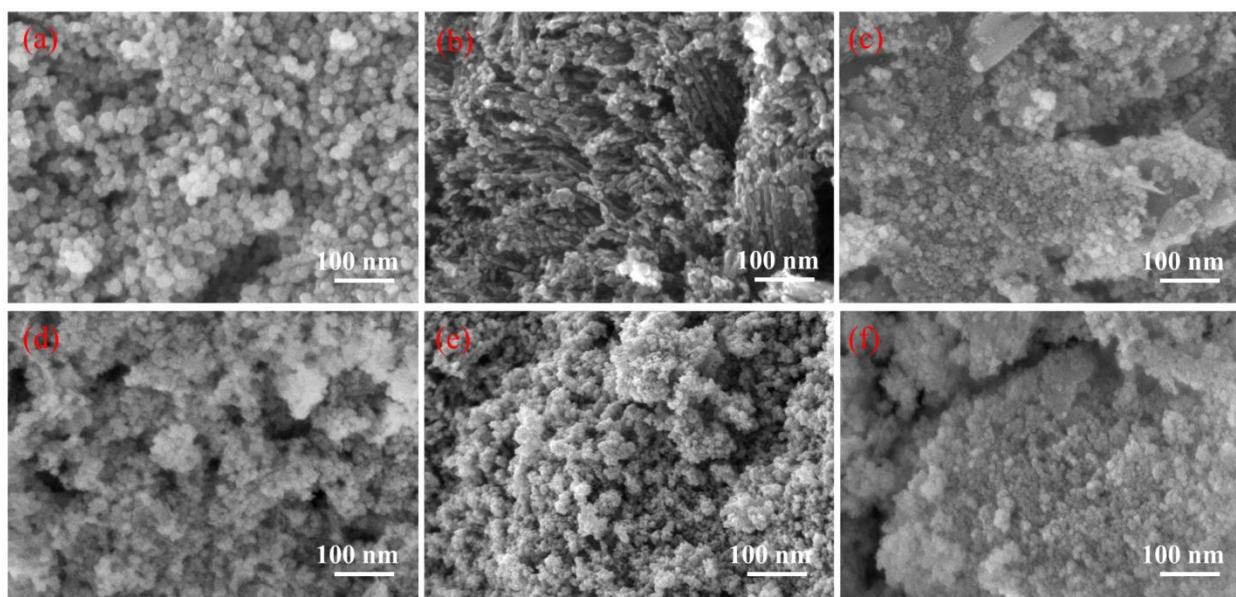


Figure S2. FESEM images of (a) 5 PGNF, (b) 10 PGNF, (c) 15 PGNF, (d) 20 PGNF, (e) 25 PGNF and (f) 30 PGNF composite.

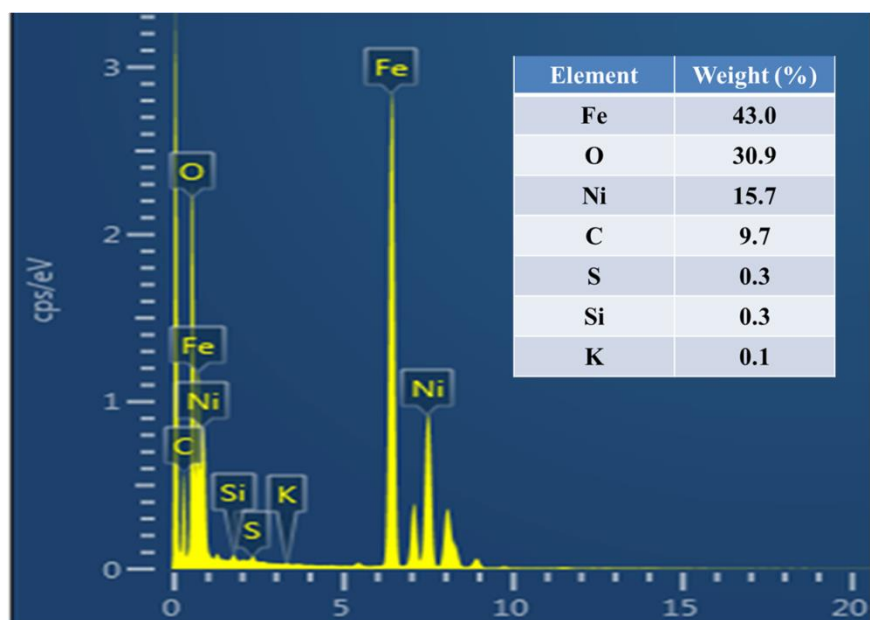


Figure S3. EDS elemental mapping of 10 PGNF.

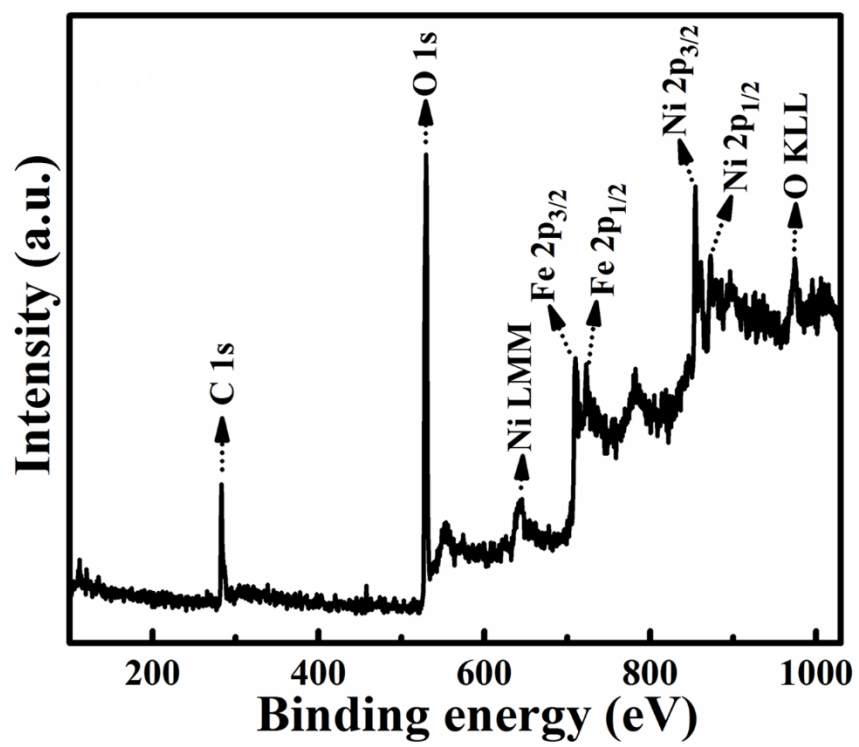


Figure S4. XPS survey spectrum of 10 PGNF composite.

Table S1. Specific capacitance values calculated for PGNF composite electrodes from CV.

Sample name	Scan rate (mV s ⁻¹)	Specific capacitance (F g ⁻¹)
5 PGNF	5	753.0
	10	594.0
	20	481.0
	30	408.0
	50	335.0
10 PGNF	5	1465.0
	10	1266.0
	20	1121.0
	30	876.0
	50	563.0
15 PGNF	5	1074.0
	10	945.0
	20	847.0
	30	727.0
	50	490.0
20 PGNF	5	944.0
	10	836.0
	20	757.0
	30	562.0
	50	395.0
25 PGNF	5	524.0
	10	473.0
	20	440.0
	30	403.0
	50	315.0
30 PGNF	5	374.0
	10	343.0
	20	319.0

	30	282.0
	50	255.0

Table S2. Specific capacitance and capacity values calculated for PGNF composite electrodes from GCD.

Sample name	Current density ($A\ g^{-1}$)	Specific capacitance ($F\ g^{-1}$)	Specific capacity ($C\ g^{-1}$)
5 PGNF	1	541	243.5
	2	526	236.7
	4	452	203.4
	6	364	163.8
	8	304	136.8
	12	299	134.6
	16	263	118.4
	20	208	93.6
10 PGNF	1	1320	594.0
	2	1227	552.2
	4	1129	508.1
	6	1107	498.2
	8	1084	487.8
	12	987	444.2
	16	889	400.1
	20	800	360.0
15 PGNF	1	991	446.0
	2	756	340.2
	4	552	248.4
	6	456	205.2
	8	402	181.0
	12	372	167.4
	16	320	144.0
	20	278	125.1
20 PGNF	1	653	293.9
	2	578	260.1
	4	487	219.2

	6	403	181.4
	8	369	166.1
	12	327	147.2
	16	302	135.9
	20	251	113.0
25 PGNF	1	303	136.4
	2	261	117.5
	4	236	106.2
	6	205	92.3
	8	183	82.4
	12	157	70.7
	16	141	63.5
	20	133	59.9
30 PGNF	1	237	106.7
	2	196	88.2
	4	156	70.2
	6	140	63.0
	8	129	58.1
	12	115	51.8
	16	107	48.2
	20	97	43.7

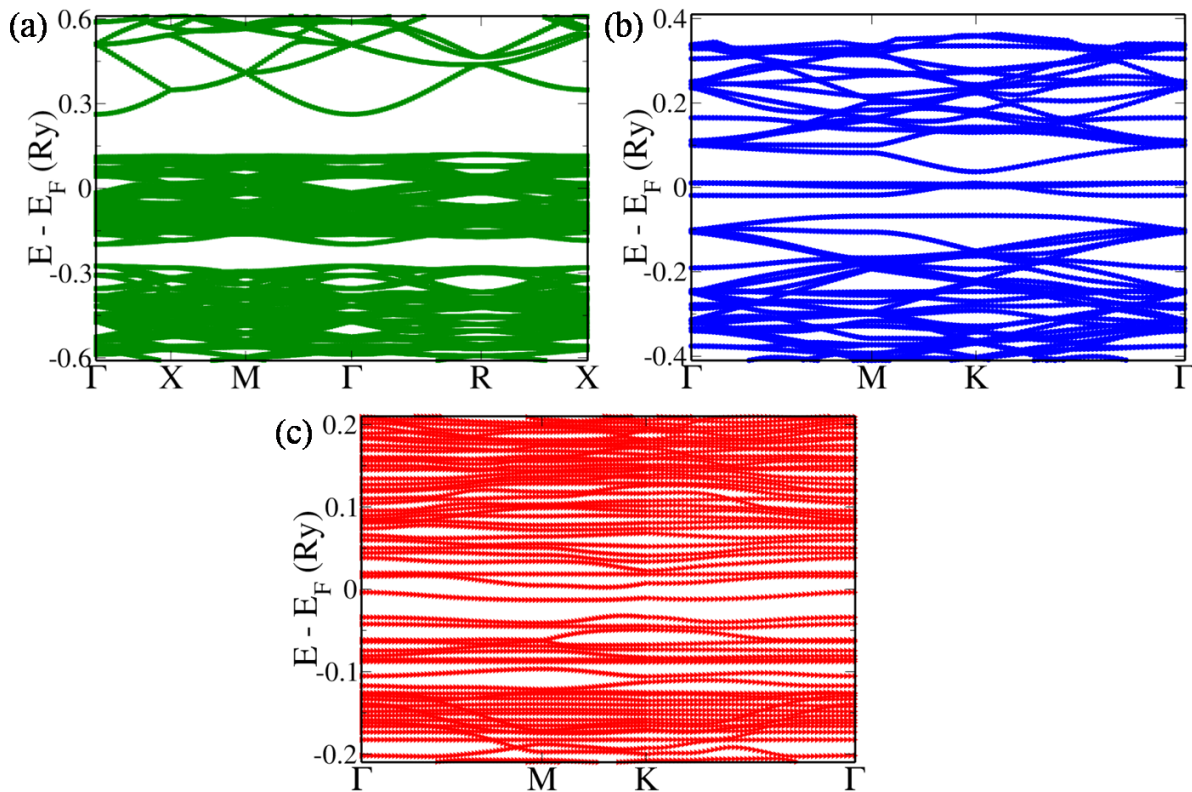


Figure S5. Electronic structure of NF, PG and PGNF. The energies are shifted with respect to the Fermi level which is set to zero.

Electronic structure of PGNF was determined to study the effect of compositing of NF with PG. Electronic structures of NF, PG and PGNF was determined using Quantum ESPRESSO package.¹ The first principles density functional theory based calculations used Perdew, Burke, and Erzenhoff pseudopotentials with $3d^84s^2$, $3d^64s^2$, $2s^22p^4$, $2s^22p^2$ configurations as valence electrons for Ni, Fe, O and C, respectively.² An inverse spinel structure for NF, a $5 \times 5 \times 1$ supercell for PG and the composite of the two was considered for the simulations. The electronic structures were determined along the high symmetry points of the Brillouin zone for the fully relaxed crystal structures. The wave functions were terminated with an energy cutoff of 50 Ry and charge density cutoff of 400 Ry. The electronic structure of NF reveals a dense valence band and conduction band on either side of Fermi level which becomes diffuse as we move further (Figure S5a). The occupation of states in the Fermi area is known to result in increased quantum capacitance. The drawback of NF is the lower pseudocapacitance.³ PG is known to possess high surface area with a favorable quantum capacitance as the electronic structure

reveals higher number of occupied states at the Fermi level in comparison to pristine graphene (Figure S5b).⁴ PGNF has increased pseudocapacitance owing to the increased surface area contributed by the porous structure of PG as revealed by the BET results. The electronic structure reveals that the states at the Fermi level still maintains the occupation leading to increased conductivity as seen in the experimental results finally leading to increased quantum capacitance (Figure S5c). The resultant of serial combination of double layer capacitance and quantum capacitance is the total capacitance of the material. Hence, we see an increase in the total capacitance in the composite compared to its constituents.

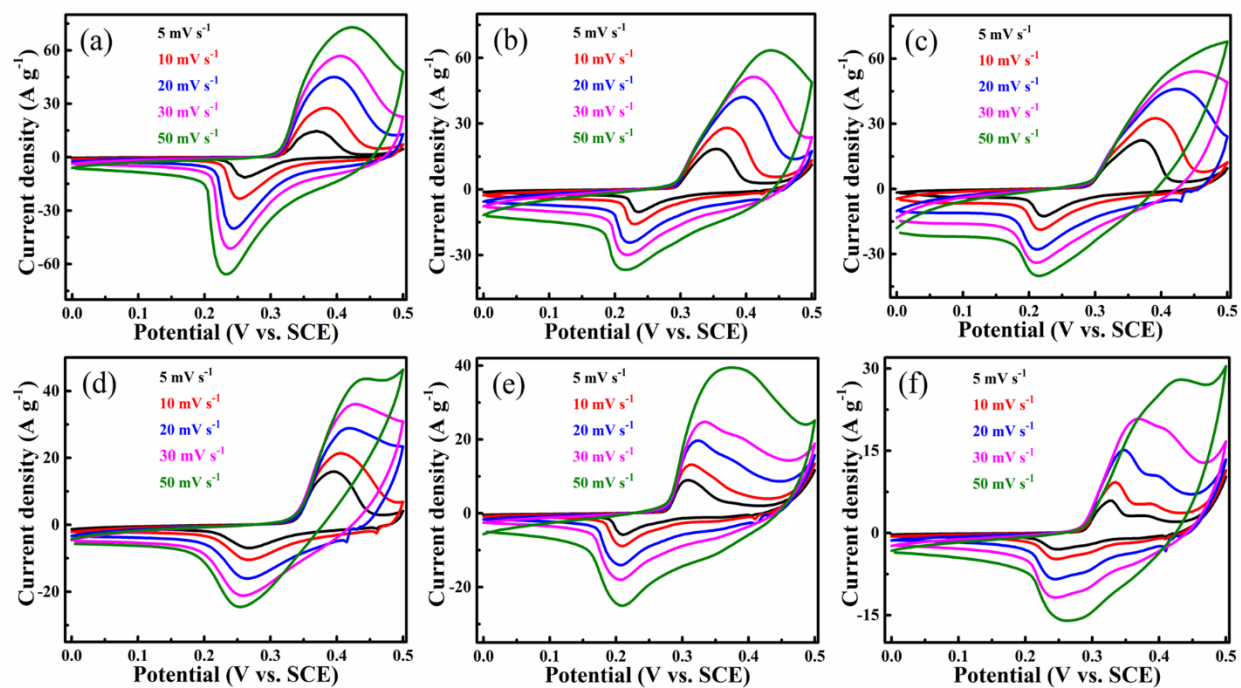


Figure S6. CV curves for (a) 5, (b) 10, (c) 15, (d) 20, (e) 25 and (f) 30 PGNF composite.

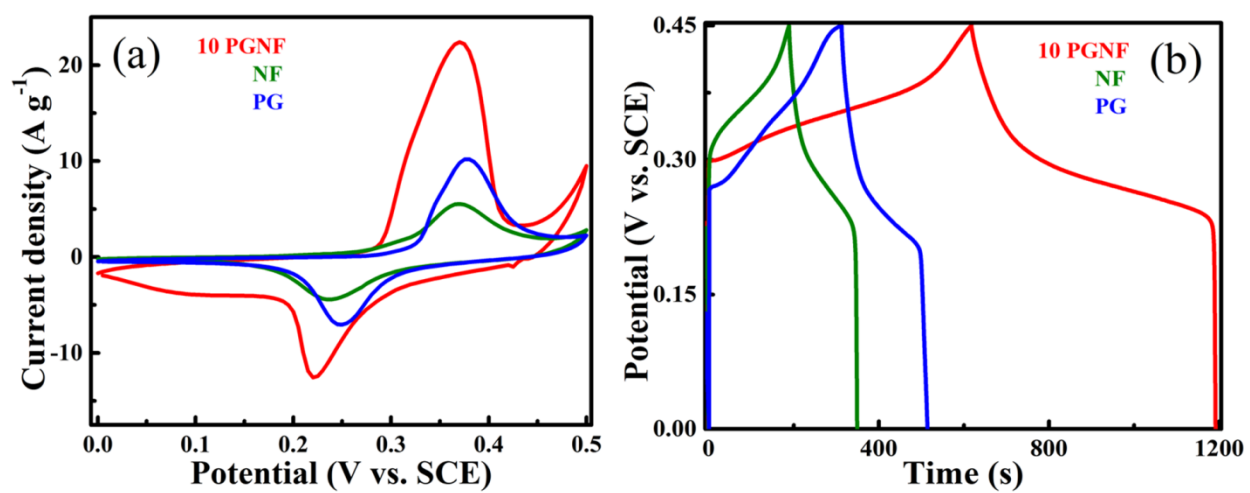


Figure S7. Comparison of electrochemical performance of NF, PG and 10 PGNF in a 3-electrode method (a) CV curves at a constant scan rate of 5 mV s^{-1} and (b) GCD curves at a constant current density of 1 A g^{-1} .

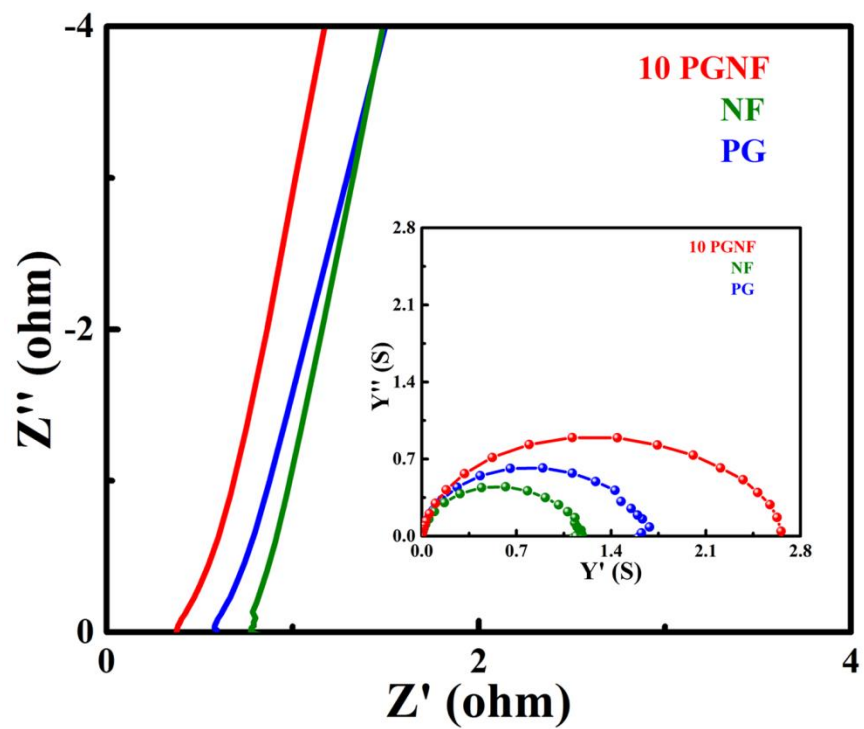


Figure S8. Comparison of Nyquist and admittance plots (inset) of NF, PG and 10 PGNF in a 3-electrode method.

Table S3. Comparison of electrochemical property parameters of NF, PG and 10 PGNF.

Electrode material	NF	PG	10 PGNF
Resistance (ohm)	0.78	0.62	0.38
Conductance (S)	1.28	1.61	2.63
Knee Frequency (kHz)	2.51	6.31	39.8
Time constant (μ s)	400.0	158.4	25.1

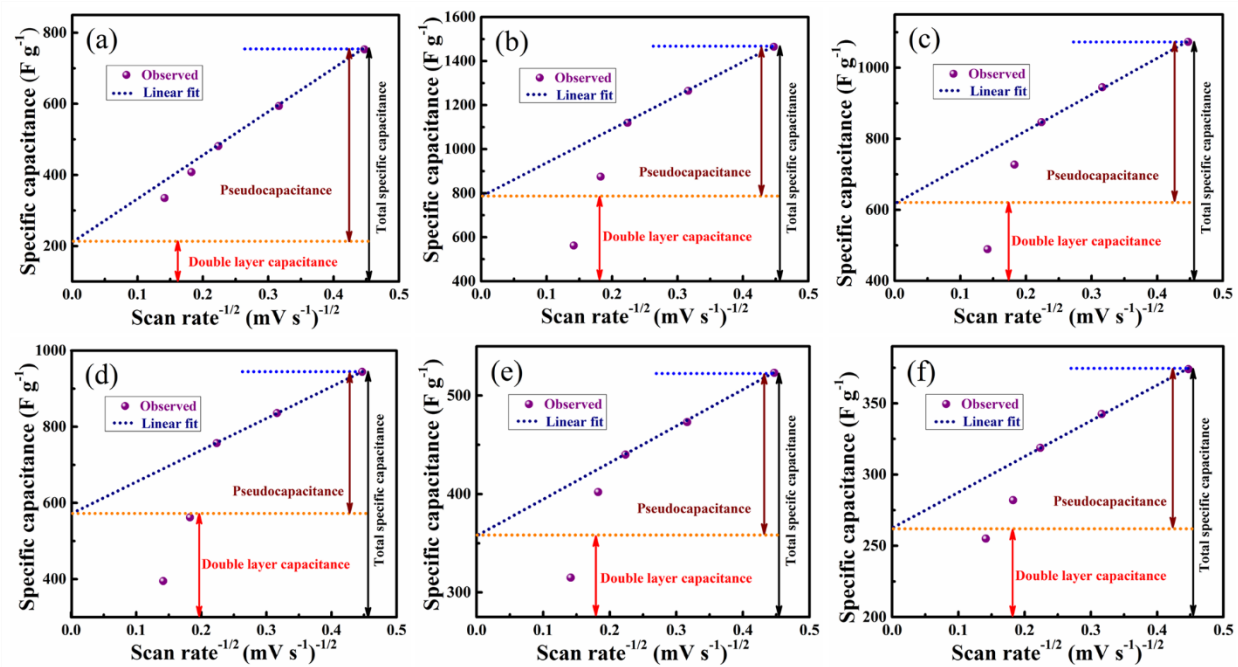


Figure S9. Determination of the double layer and pseudocapacitance contribution. Specific capacitance vs. inverse square root of scan rate of (a) 5, (b) 10, (c) 15, (d) 20, (e) 25 and (f) 30 PGNF composite. The low scan rate points are considered for fitting and high scan rate points are excluded. The intercept obtained by extrapolating the fitted curve towards the Y-axis, which provides the double layer capacitance and the subtraction of double layer contribution from the total capacitance gives the pseudocapacitance contribution.

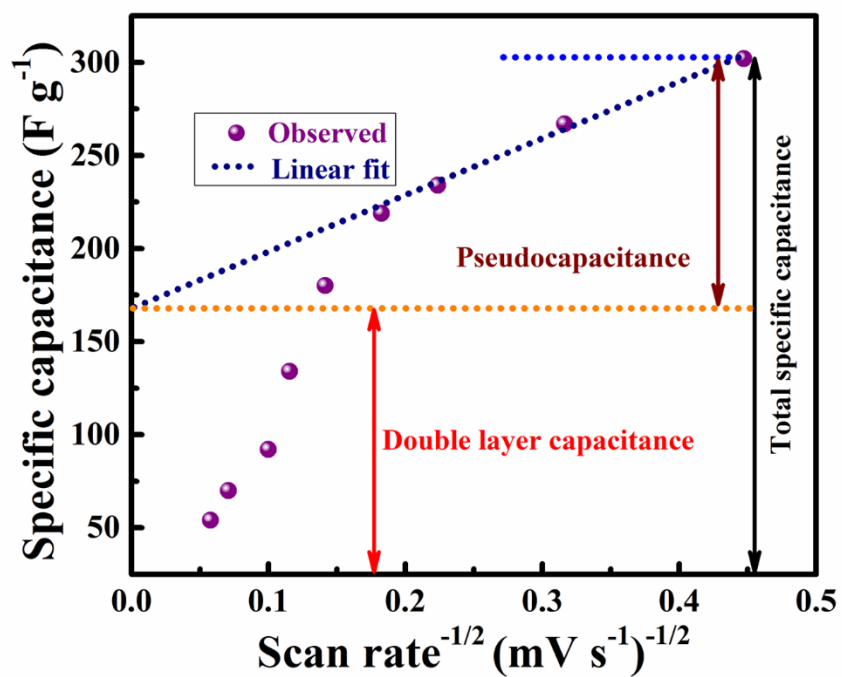


Figure S10. Determination of the double layer and pseudocapacitance contribution. Specific capacitance vs. inverse square root of scan rate of the fabricated symmetrical supercapacitor device.

Table S4. Comparison of electrochemical performance of the 10 PGNF with other reported literatures for electrode and fabricated device.

Electrode material/ fabricated device	Specific Capacitance ($F g^{-1}$) from CV data ($mV s^{-1}$)	Specific Capacitance ($F g^{-1}$) from GCD data ($A g^{-1}$)	Electrolyte	Cyclic stability	Reference
PGNF electrode	1465 @ 5 $mV s^{-1}$	1320 @ 1 $A g^{-1}$	2 M KOH	94 % after 10000 cycles (8 $A g^{-1}$)	This work
Cu substituted NF @Graphene sheet electrode	----	735 @ 1.47 $mA g^{-1}$	1 M KOH	85% after 1000 cycles	Bashir et al. (2019) ⁵
NF@RGO electrode	----	215.7 @ 0.5 $A g^{-1}$	1 M Na_2SO_4	89.4% after 10000 cycles (10 $A g^{-1}$)	Cai et al. (2019) ⁶
NF@RGO electrode	----	488 @ 1 $A g^{-1}$	PVA- KNO_3 electrolyte	89.8 % after 10000 cycles (3 $A g^{-1}$)	Zhang et al. (2019) ⁷
PGNFdevice	303 @ 5 $mV s^{-1}$	160 @ 4 $A g^{-1}$	2 M KOH	96 % after 10000 cycles (8 $A g^{-1}$)	This work
NF@Graphene device	----	481 @ 0.1 $A g^{-1}$	6 M KOH	99 % after 10000 cycles (1 $A g^{-1}$)	Fu et al. (2018) ⁸
NF@CNT device	66 @ 5 $mV s^{-1}$	----	2 M KOH	79 % after 2500 cycles (2	Kumar et al. (2018) ⁹

				A g ⁻¹)	
NF@RGode vice	----	121 @ 0.5 A g ⁻¹		93.2 % after 6000 cycles (3 A g ⁻¹)	Zhang et al. (2019) ⁷
NF@Graphe ne device	3.1 @ 100 mVs ⁻¹	---	1 M Na ₂ SO ₄	---	Soam et al. (2020) ¹⁰

References

1. P. Giannozzi, S. Baroni, N. Bonini, M. Calandra, R. Car, C. Cavazzoni, D. Ceresoli, G. L. Chiarotti, M. Cococcioni and I. Dabo, et al., *J. Phys.: Condens. Matter*, 2009, **21**, 395502.
2. J. P. Perdew, K. Burke and M. Ernzerhof, *Phys. Rev. Lett.*, 1996,**77**, 3865-3868.
3. M. Sethi, S.U. Shenoy, M. Selvakumar and D.K. Bhat, *Front. Mater. Sci.*, 2020,**14**,120-132.
4. M. Sethi, H. Bantawal, S.U. Shenoy and D.K. Bhat, *J. Alloys Compd.*, 2019, **799**, 256-256.
5. B. Bashir, A. Rahman, H. Sabeeh, M.A. Khan, M.F.A. Aboud, M.F. Warsi, I. Shakir, P.O. Agboola and M. Shahid, *Ceram. Int.*,2019, **45**, 6759-6766.
6. Y.Z. Cai, W.Q. Cao, P. He, Y.L. Zhang and M.S. Cao, *Mater. Res. Express*, 2019, **6**, 105535.
7. X. Zhang, M. Zhu, T. Ouyang, Y. Chen, J. Yan, K. Zhu, K. Ye, G. Wang, K. Cheng and D. Cao, *Chem. Eng. J.*, 2019, **360**, 171-179.
8. M. Fu, W. Chen, X. Zhu and Q. Liu, *J. Power Sources*, 2018, **396**, 41-48.
9. N. Kumar, A. Kumar, G.M. Huang, W.W. Wu and T.Y. Tseng, *Appl. Surf. Sci.*, 2018, **433**, 1100-1112.
10. A. Soam, R. Kumar, D. Thatoi and M. Singh, *J. Inorganic Organometallic Polymers Mater.*, 2020, DOI:<https://doi.org/10.1007/s10904-020-01540-7>.